Appl. Phys. B 79, 497–501 (2004)
DOI: 10.1007/s00340-004-1596-1

Applied Physics B
Lasers and Optics

V.V. KRISHNAMACHARI✉
C. DENZ

A phase-triggering technique to extend the phase-measurement range of a photorefractive novelty filter microscope

Institut für Angewandte Physik, Westfälische Wilhelms-Universität, Corrensstrasse 2/4, 48149 Münster, Germany

Received: 16 January 2004/Revised version: 16 June 2004
Published online: 22 July 2004 • © Springer-Verlag 2004

ABSTRACT A photorefractive-based novelty filter microscope can be used for real-time phase measurement of phase changes, introduced by moving objects or microorganisms, from 0 to π radians. In this article, we propose a method to extend the phase-measurement range over the entire 2π radians and demonstrate its validity both experimentally and numerically. Our method makes use of the fact that the slopes of the calibration curve of the novelty filter microscope in the positive- and the negative-phase regions have opposite signs. By applying a known external phase trigger to the novelty filter system, the positive- and negative-phase regions can be differentiated.

PACS 07.60.Pb; 42.30.-d; 42.65.Hw

1 Introduction

The photorefractive novelty filter based microscope (NFM), first proposed by Cudney et al. [2], can detect changes in the amplitude and the phase of the incident beam [3]. The amplitude sensitivity of the device has often been used by many authors to perform object tracking, image subtraction, image differentiation, object comparison and contour generation [4–10]). On the other hand, its real-time phase sensitivity has remained relatively unexploited. Sedlatschek et al. [11] made the first effort in showing that a photorefractive-based novelty filter has a characteristic phase-transfer function (PTF). A simple expression for the PTF based on the undepleted pump approximation was derived by Delaye and Roosen [12]. The PTF shows the dependence of the novelty filter output (NFO) intensity on the input phase change. We demonstrated that it can be used to measure two-dimensional phase changes in the range of 0 to π radians in real time [1]. We showed that it involves two steps. The first step is the suppression of the trail formation [13, 14] in the novelty filter output. This we achieved by exploiting the intensity dependence of the photorefractive time constant. By choosing a large time constant, the detected two-dimensional novelty filter output shows one-to-one correspondence to the input with minimal trail formation. The second step involves calibrating the novelty filter microscope setup using a phase-only modulating liquid-crystal display. The resulting PTF can be used to create a look-up table to match the detected CCD gray level to the corresponding phase-change value.

The main emphasis of this article is to propose and experimentally demonstrate a method to extend the phase-measurement range over the entire 2π radians. The phase-transfer function of the novelty filter is not a one-to-one function over the phase range of $-\pi$ to $+\pi$ radians. Hence, the detected output at the CCD camera cannot be uniquely mapped to a single phase-change value. Here, we propose a technique to overcome this problem. This technique uses the fact that the slopes of the PTF have different signs in the positive- and the negative-phase regions. In Sect. 2, we present our microscope system and the calibration curve of the filter. In Sect. 3, we discuss in detail the idea behind the method to extend the phase-measurement range. We describe the experimental realization of the method and present our experimental and numerical results. We also present a brief discussion on the further consequences of using this method with regard to the phase-measurement resolution.

2 Novelty filter microscope and PTF

Figure 1 shows the experimental sketch of our novelty filter microscope system. The laser beam from a frequency-doubled Nd:YAG laser is split into a signal beam and a reference beam. The extra-ordinarily polarized signal beam illuminates the probe, which in our case is a phase-modulating liquid-crystal display (LCD). The LCD has a pixel pitch of 36 μm and a resolution of 800×600 pixels. It can be controlled from the VGA output of any desktop computer. This LCD is viewed with the help of a microscope objective in conjunction with a projecting lens system and a progressive-scan CCD camera. The reference beam, with the right polarization, is made to interfere with the signal beam in a photorefractive $BaTiO_3$ crystal. The crystal is oriented in such a way that the signal beam loses energy to the reference beam with a two-wave-mixing time constant of 20 s.

We determined the PTF of the system by letting pixel clusters of different phase values, generated on the LCD, move across the field of view of the microscope and detecting the output at the CCD. Figure 2a shows the curve for the phase range from $-\pi$ to π radians and it represents the characteristic

✉ Fax: +49-251/833-3513, E-mail: vishnu@uni-muenster.de

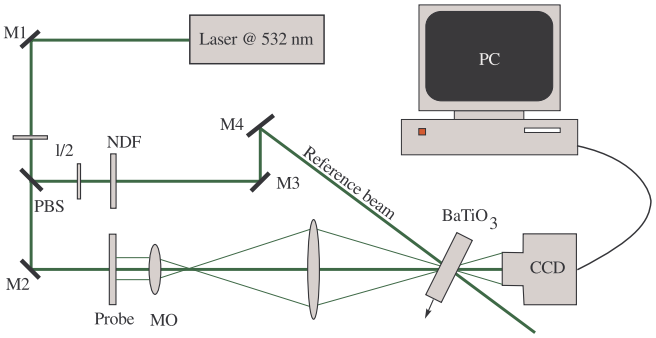

FIGURE 1 Experimental setup of the novelty filter microscope

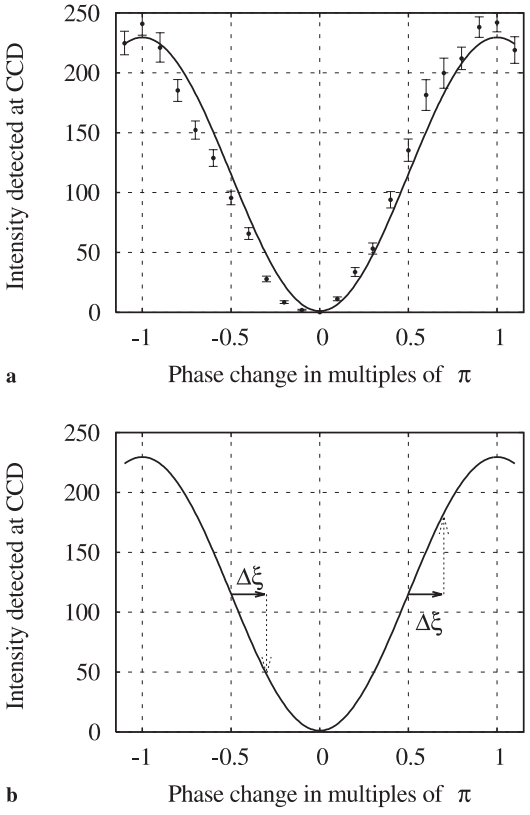

FIGURE 2 **a** The phase-transfer function of the novelty filter microscope. **b** Extending the phase-measurement range: an idea

curve of the novelty filter microscope system. As is evident, this curve is not a one-to-one function. The output intensity detected at the CCD camera gives information only about the magnitude of the input phase change but not about the sign of the phase change. To overcome this ambiguity, a new method has to be devised to map the detected output to the corresponding input phase change.

3 Extension of the phase-measurement range

We present a simple but effective technique to extend the phase-measurement range of the novelty filter microscope over the entire 2π radians. This technique exploits the fact that the slopes of the PTF have opposite signs in the positive (between $2n\pi$ and $2n\pi+\pi$) and the negative (between $2n\pi-\pi$ and $2n\pi$) phase regions. The idea behind our technique is to apply a known, small phase trigger of $\Delta\xi$ to the signal beam as a phase object, whose phase distribution needs to be determined, moving across the field of view. In this article we consider applying a positive phase trigger to the signal beam. From the PTF, it is to be expected that the positive-phase regions should get brighter and the negative-phase regions should get darker. This idea is schematically shown in Fig. 2b.

3.1 *Experimental implementation*

The experimental implementation of the external phase triggering of the novelty filter system, as shown in Fig. 2b, requires the application of a positive phase trigger of $\Delta\xi$ to the entire signal beam. Applying an external trigger to the signal beam is not practicable, as the signal beam is mostly an expanded laser beam containing important two-dimensional information. Instead, the phase of the unexpanded reference beam in the two-beam-coupling novelty filter system can be easily modified. However, in such a case, the phase trigger to be applied to the reference beam should be negative ($-\Delta\xi$ radians). This can be understood if one considers the fact that the hologram stored in the photorefractive crystal contains the information about the difference between the phases of the signal and the reference beams. Because of this, applying an extra phase change of $+\Delta\xi$ to the signal beam is equivalent to introducing a phase change of $-\Delta\xi$ to the reference beam.

One of the simplest techniques to modify the phase of a beam is to use the reflected light of the beam from a moving mirror. To incorporate this idea in our novelty filter system, we replaced the stationary mirror M4 in the reference arm with a computer-controlled piezo mirror. Before this mirror was integrated in the experimental setup, we calibrated it interferometrically to determine the dependence of the optical path difference introduced in the reflected light on the applied voltage. Using this mirror, we could introduce a phase trigger of -0.2π radians in the reference beam. We chose this value of phase trigger to effectively use the complete dynamic range of the CCD camera and also to be able to resolve phase shifts of 0.1π radians.

To test the validity of our technique, we performed experiments with moving pixel clusters generated using the LCD in the field of view of the microscope system. To easily verify the effectiveness of the technique, we let a pixel cluster of 6×6, whose configuration is shown in Fig. 3, move from left to right across the field of view of the microscope with a speed of 20 pixels/s. In this pixel cluster, the phase of the top three rows is positive with respect to the background and the phase of the bottom three rows is negative. Along each column of the cluster, the magnitude of the phase is the same. The experimental results obtained using this technique will be compared with the numerical results in Sect. 3.3.

The idea of applying an external phase trigger to determine the phase changes is often used in the field of phase-shifting interferometry (PSI) to study the motion of diffusely reflecting objects [16]. Though the NFM technique presented in this article and PSI may have the similarity of using an external phase trigger, they have significant differences. In PSI, firstly, the initial configuration of the signal beam is recorded in a holographic medium. In the second stage of measurement,

0	0.1π	0.2π	0.3π	0.4π	0.5π
0	0.1π	0.2π	0.3π	0.4π	0.5π
0	0.1π	0.2π	0.3π	0.4π	0.5π
0	-0.1π	-0.2π	-0.3π	-0.4π	-0.5π
0	-0.1π	-0.2π	-0.3π	-0.4π	-0.5π
0	-0.1π	-0.2π	-0.3π	-0.4π	-0.5π

FIGURE 3 Phase pixel cluster to test the validity of the phase-triggering technique

this hologram is read out with three or four or sometimes five successive and mostly equally phase-shifted reference beams. Each time, the new configuration of the signal beam is made to interfere with the diffracted portion of the reference beam. The resulting set of interferograms are mathematically processed to obtain the change in the phase of the signal beam. The technique of PSI was also realized using the Bismuth Silicon Oxide (BSO) photorefractive crystal [17]. The NFM technique presented in this article has many points of contrast. The more important ones are listed below.

- In the NFM technique, at the output one does not obtain an interferogram but rather an image of the object under investigation. This makes it quite simple to analyze the captured image frames without any requirement for mathematical processing of the interference fringes and subsequent phase-unwrapping strategies. In this method, the detected gray values at the CCD camera can be directly converted to phase changes using the previously determined look-up table.
- In PSI, during one cycle of measurement which involves successive application of four phase shifts to the reference beam and subsequent capture of images, the object under investigation should not move or undergo any change. This presents a strong limitation on the speed with which the measurements can be made. In the NFM method, even during the presence of the trigger, the object can deform or undergo motion. Thus the speed of phase measurement using the novelty filter microscope is only limited by the speed of acquisition of the camera or any other image-registering device.
- Another major difference between the two techniques is the number of required phase shifts. In the PSI technique, a minimum of three and most often four phase-shifted interferograms are required. This is because in this technique one detects the interference fringes. In any given region of the output there are a minimum of three unknown variables corresponding to the average fringe intensity, the fringe-modulation amplitude and the phase difference between the two states of the signal beam. In the NFM technique, only one phase shift or trigger needs to be applied. Due to the direct imaging of the object, the only unknown parameter is its phase distribution. However, the intensity output detected at the CCD camera shows an ambiguity for negative and positive phase changes and, to remove this ambiguity, one novelty filtered image obtained during the presence of a phase trigger is required.
- In the NFM method, one detects only the transient phase changes. That is, to measure the phase distribution of a phase object, it has to be in motion under the field of view of the NFM. However, with PSI one can make measurements on stationary phase objects and determine their phase distributions.

3.2 *Numerical simulations*

In addition to the experimental investigations, we performed numerical calculations to test the validity of our method. The aim of this exercise was to confirm that the experimental results obtained by us were not related to any artifacts particular to our experimental setup but rather based on the predictions of the existing theory of the photorefractive effect. The starting equations in our numerical simulations are the coupled wave equations [15] of two beams, with complex amplitudes $\mathcal{A}_{\text{sig}}$ and $\mathcal{A}_{\text{ref}}$, diffracting from a photorefractive grating in a diffusion-dominated crystal.

$$\frac{\mathrm{d}}{\mathrm{d}z}\mathcal{A}_{\text{sig}} = -\mathcal{G} \times \mathcal{A}_{\text{ref}}, \tag{1}$$

$$\frac{\mathrm{d}}{\mathrm{d}z}\mathcal{A}_{\text{ref}} = \mathcal{G}^* \times \mathcal{A}_{\text{sig}}. \tag{2}$$

In the above equations, $\mathcal{G}$ is the grating amplitude in the photorefractive crystal. Since the photorefractive grating is continuously modified by the incident beams, its time evolution can be written as

$$\frac{\partial}{\partial t}\mathcal{G} = -\frac{1}{\tau}\left[\mathcal{G} - \frac{\Gamma \mathcal{A}^*_{\text{ref}}\mathcal{A}_{\text{sig}}}{2I_0}\right], \tag{3}$$

where

$$\Gamma = \mathrm{i}\frac{2\pi n_1}{\lambda \cos\theta}\mathrm{e}^{-\mathrm{i}\varphi}, \tag{4}$$

and I_0 is the total intensity and τ is the time constant for grating formation or erasure.

The reason for choosing this complex depleted-pump model rather than the simplified undepleted pump approximation models is to keep the numerics as general as possible. In our simulations, we assume that the signal and the reference beams at t_0, $\mathcal{A}_{\text{sig}}(z = 0, t = t_0)$ and $\mathcal{A}_{\text{ref}}(z = 0, t = t_0)$, have been presented to the novelty filter since $t = -\infty$, so that the grating corresponding to this signal- and reference-beam configuration is written in the crystal for the entire length of the crystal d. This initial grating can be easily calculated by letting the time derivative in (3) go to zero. With the initial grating known, the first-order coupled-wave equations (1) and (2) were solved using the fourth-order Runge–Kutta method. The resulting wave amplitudes were used in (3) to calculate the new grating amplitude, which in turn was inserted in the wave equations to calculate the new wave amplitudes for the next time step. This process was repeated for all the time

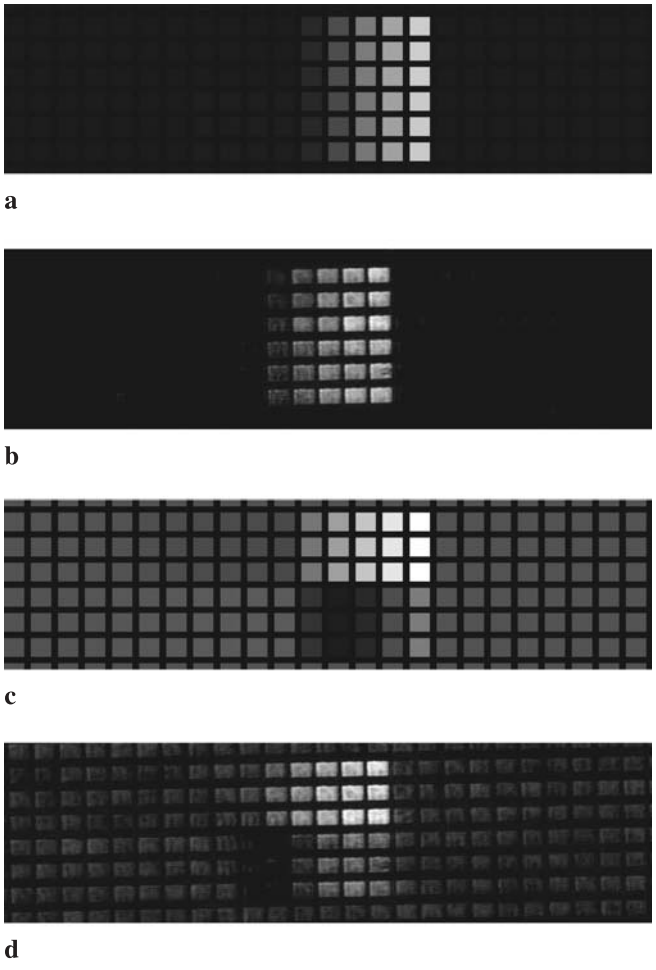

FIGURE 4 Novelty filter microscope output in the absence (**a**, **b**) and in the presence (**c**, **d**) of external phase trigger of -0.2π radians: simulation (**a**, **c**) and experimental (**b**, **d**) results

steps and for all the transverse coordinates to obtain the two-dimensional novelty filtered output.

In our simulations, the transverse areas of the signal and the reference beams were discretized into a matrix of 48 rows and 96 columns. The two-dimensional input to our simulation program was chosen to look 'similar' to the input to our experimental setup. The word 'similar' needs some more explanation. The LCD used in our experiments has opaque regions interspersing the active pixels. This can be clearly seen in Fig. 4d. To qualitatively compare the experimental observations in Fig. 4b and d, we chose an input for our numerical calculations that has 'opaque' regions interspersing the 'active' regions whose amplitude can be changed. The novelty filtered output was determined from 0 to 1 s in steps of 25 ms. As numerical parameters, $\tau = 20$ s, $\varphi = 90°$ (the phase shift between the refractive index and the interference gratings) and $\lambda = 532$ nm were used.

3.3 *Results and discussion*

The results from the numerical calculations and those from the experiment are compared in Fig. 4. Figure 4a and b show the calculated and the detected novelty filtered outputs, respectively. Clearly, the positive- and the negative-

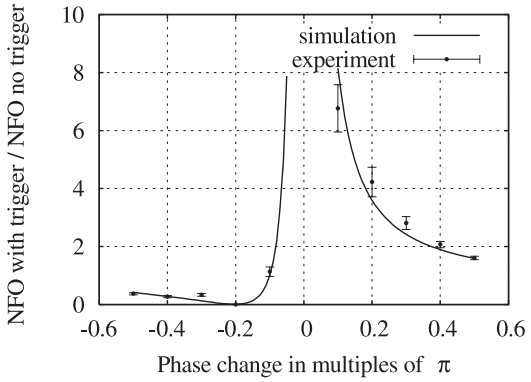

FIGURE 5 Input phase change versus the ratio between the novelty filter output (NFO) in the presence of the external phase trigger of -0.2π radians and that during the absence of the phase trigger: a comparison between the theory and the experiment

phase regions cannot be differentiated. This is to be expected as the novelty filter microscope characteristic curve is not a one-to-one function as explained in Sect. 3.1. Figure 4c and d show the result when an external phase trigger of -0.2π radians is applied to the reference beam. From the figure, it is evident that the positive-phase regions look brighter and the negative-phase regions darker.

Apart from good qualitative agreement between the simulation and the experiment, we could also obtain a good quantitative agreement. This is best depicted in Fig. 5, which shows a plot of the ratio between the novelty filtered output during the presence of the trigger and that during the absence of the trigger with respect to the input phase change. Clearly, there is an excellent agreement between the theoretical predictions and the experimental observations. Thus, by applying an external phase trigger, the positive- and the negative-phase regions can be differentiated.

In our experiments, the duration of the phase trigger was set to 300 ms, which is much smaller than the grating formation time of 20 s. However, the minimum duration ($\tau_{\min}^{\mathrm{PT}}$) of the application of the phase trigger could be just long enough to capture a single image frame in the presence of the phase trigger. For example, if the camera used to capture images operates at 30 frames per second, then $\tau_{\min}^{\mathrm{PT}}$ is 66.7 ms (with no synchronization between the camera and the phase-triggering element). The maximum phase-trigger duration ($\tau_{\max}^{\mathrm{PT}}$) is limited by the grating formation time of the photorefractive crystal. By requiring that during the presence of the trigger the decrease in the output intensity should be less than 5% of its initial value, which corresponds to a change of 13 gray levels for an 8-bit camera, $\tau_{\max}^{\mathrm{PT}}$ can be calculated. If the novelty filtered output is assumed to be exponentially varying and if the intensity output as soon as the phase trigger occurs is taken to be unity, then the intensity output after a duration of $\tau_{\max}^{\mathrm{PT}}$ is given by $\exp(-\tau_{\max}^{\mathrm{PT}}/\tau)$. Then, from the above constraint, we have

$$\tau_{\max}^{\mathrm{PT}} < 0.05\tau. \tag{5}$$

Another important consequence of using this technique is that it enables measurement of phase changes close to 0, $-\pi$ and $+\pi$ radians with improved accuracy. To substantiate this

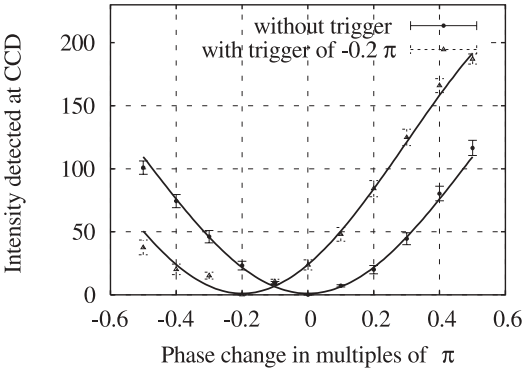

FIGURE 6 PTF in the presence (*triangles*) and in the absence (*solid circles*) of the external phase trigger to the reference beam

point, we determined the phase-transfer function of the system in the presence and in the absence of the external phase trigger, which is plotted in Fig. 6. The phase-measurement resolution of the novelty filter microscope is not uniform over the entire phase-measurement range. For small phase changes and for phase changes close to $-\pi$ and $+\pi$ radians, the measurement resolution deteriorates. This can be clearly seen from the curve which corresponds to the case when no trigger was applied. The PTF of the system during the application of the trigger is phase shifted by -0.2π radians. This was done by calculating the average gray value in different phase regions of the object. From this curve, it is evident that the phase changes of 0.1π and 0.2π can be better resolved compared to the case when no external phase trigger was applied.

Though our experiments were restricted to the investigation of simple horizontal motion of pixel clusters with a constant velocity, the technique presented here can be readily used to analyze the phase distribution of objects that are accelerating or performing complex motion. The first step in the phase-determining process is to associate the correct magnitude of the phase in the different regions of the object by mapping the detected gray value to the corresponding phase value. This is achieved using the look-up table determined while calibrating the system. The second step is to use the information provided by the images captured during the presence of the phase trigger. Towards this end, the moving phase objects should be tracked using efficient image-processing operations. Once this is done, it is straightforward to determine the regions that get darker in the phase-triggered images (assuming that a negative phase trigger was applied to the reference beam) and to associate the negative sign to the phase value in that region.

4 Conclusion

The work presented in this article is an important step forward towards operating the photorefractive novelty filter microscope as an all-optical transient phase measuring device over the entire range of 2π radians. Here, we presented a technique to extend the phase-measurement range of the photorefractive novelty filter microscope. This technique makes use of the fact that the slopes of the phase-transfer function of the microscope have opposite signs in the positive- and the negative-phase regions. We investigated the validity of this technique both experimentally and numerically. We also showed that, using this method, the regions with phase changes close to zero and $\pm\pi$ radians can be resolved with better accuracy.

REFERENCES

1 V.V. Krishnamachari, C. Denz: J. Opt. A **5**, S239 (2003)
2 R.S. Cudney, R.M. Pierce, J. Feinberg: Nature **332**, 424 (1988)
3 D.Z. Anderson, J. Feinberg: IEEE J. Quantum Electron. **QE-25**, 635 (1989)
4 D.Z. Anderson, D.M. Lininger, J. Feinberg: Opt. Lett. **12**, 123 (1987)
5 N.S.-K. Kwong, Y. Tamita, A. Yariv: J. Opt. Soc. Am. B **5**, 1788 (1988)
6 J.A. Khoury, G. Hussain, R.W. Eason: Opt. Commun. **71**, 138 (1989)
7 C. Soutar, C.M. Cartwright, W.A. Gillespie, Z.Q. Wang: Opt. Commun. **86**, 255 (1991)
8 M. Sedlatschek, T. Rauch, C. Denz, T. Tschudi: Opt. Mater. **4**, 376 (1995)
9 P. Mathey, P. Jullien, A. Dazzi, B. Mazué: Opt. Commun. **129**, 301 (1996)
10 P. Mathey, B. Mazué, P. Jullien: J. Opt. Soc. Am. B **15**, 1353 (1998)
11 M. Sedlatschek, J. Trumpfheller, J. Hartmann, M. Müller, C. Denz, T. Tschudi: Appl. Phys. B **68**, 1047 (1999)
12 P. Delaye, G. Roosen: Opt. Commun. **165**, 133 (1999)
13 A. Chen, S. Fan, H. Ding, C. Wu: Appl. Opt. **33**, 2998 (1994)
14 M. Sedlatschek, T. Rauch, C. Denz, T. Tschudi: Opt. Commun. **116**, 25 (1995)
15 P. Yeh: *Introduction to Photorefractive Nonlinear Optics* (Wiley, New York 1993)
16 P. Hariharan: *Optical Holography: Principles, Techniques and Applications* (Cambridge University Press, New York 1996)
17 M.P. Georges, Ph.C. Lemaire: Appl. Opt. **34**, 7497 (1995)